

Short- and long-term dynamic responses of the metabolic network and gene expression in yeast to a transient change in the nutrient environment†

Duygu Dikicioglu,^a Warwick B. Dunn,^b Douglas B. Kell,^c Betul Kirdar^a and Stephen G. Oliver^{*ad}

Received 26th October 2011, Accepted 9th March 2012

DOI: 10.1039/c2mb05443d

Quantitative data on the dynamic changes in the transcriptome and the metabolome of yeast in response to an impulse-like perturbation in nutrient availability was integrated with the metabolic pathway information in order to elucidate the long-term dynamic re-organization of the cells. This study revealed that, in addition to the dynamic re-organization of the *de novo* biosynthetic pathways, salvage pathways were also re-organized in a time-dependent manner upon catabolite repression. The transcriptional and the metabolic responses observed for nitrogen catabolite repression were not as severe as those observed for carbon catabolite repression. Selective up- or down regulation of a single member of a paralogous gene pair during the response to the relaxation from nutritional limitation was identified indicating a differentiation of functions among paralogs. Our study highlighted the role of inosine accumulation and recycling in energy homeostasis and indicated possible bottlenecks in the process.

Introduction

The survival of a free-living microorganism depends on its ability to deal with changes in its physicochemical environment, including variations in temperature,¹ pH² or nutrient availability.^{3–8} Appropriate mechanisms to deal with such changes rapidly and effectively were developed over evolutionary time, and the expression of more than half of yeast's genes were observed to change in response to environmental perturbations.^{2,9} The mechanism underlying the sensing and utilization of glucose, which is the most abundant monosaccharide on earth and the most preferred carbon source for most organisms, are of particular importance and were studied extensively (see ref. 10).

Glucose has a central role in yeast metabolism, both as both a nutrient and a regulator. The introduction of excess glucose into the growth environment of respiring *Saccharomyces cerevisiae* cells switches metabolism to the fermentative mode, inducing various signal transduction pathways and causing several proteins to be activated or inactivated. Carbon catabolite repression is the ability of glucose to repress the expression of several genes that encode enzymes involved in gluconeogenesis, respiration, mitochondrial development, and the utilization of carbon sources other than glucose, fructose or mannose.¹¹ The regulation and control determined by the availability of glucose may be exerted at different levels; however, its main effect was reported to take place at the transcriptional level.¹² The increase in growth rate evoked by the introduction of glucose into a carbon-limited culture was observed to cause a distinctive restructuring of yeast's transcriptional profile. The Snf1-Rgt pathway was reported to have a specific, but limited, role in this response; while protein kinase A and Sch9p were reported to be responsible for triggering more than 90% of all glucose-induced changes, including those in response to the respiratory and gluconeogenic pathways.¹³ Similarly, an increase in the glucose concentration of the growth medium was associated with a pronounced drop of adenine nucleotide content and the interconversion of adenine nucleotides and inosine was proposed to provide a rapid and energetically cost-efficient mechanism of adaptation.¹⁴

Ammonium is assimilated in yeast *via* its conversion into glutamate.¹⁵ Although glutamate, itself, is the most preferred

^a Department of Chemical Engineering, Bogazici University, Bebek 34342, Istanbul, Turkey. E-mail: duygu.dikicioglu@boun.edu.tr, kirdar@boun.edu.tr; Fax: +90 212 287 2460; Tel: +90 212 359 7126

^b Manchester Centre for Integrative Systems Biology, University of Manchester, M1 7DN, Manchester, United Kingdom. E-mail: Warwick.Dunn@manchester.ac.uk; Fax: +44 161 30 64556; Tel: +44 161 30 65146

^c School of Chemistry and Manchester Interdisciplinary Biocentre, University of Manchester, M1 7DN, Manchester, United Kingdom. E-mail: dbk@manchester.ac.uk; Fax: +44 161 306 4556; Tel: +44 161 306 4492

^d Cambridge Systems Biology Centre & Department of Biochemistry, University of Cambridge, CB2 1GA, Cambridge, United Kingdom. E-mail: steve.oliver@bioc.cam.ac.uk; Fax: +44 1223 766 002; Tel: +44 1223 333 667

† Electronic supplementary information (ESI) available: See DOI: 10.1039/c2mb05443d

nitrogen source for the organism, laboratory strains of yeast grow very well on ammonium as the principal source of nitrogen.¹⁶ Thus, on ammonium-based media, yeast cells were reported to decrease the activities of enzymes involved in the utilization of poor nitrogen sources—a phenomenon termed nitrogen catabolite repression. The cellular response to sudden changes in the amount of available ammonium has received much less attention from researchers than the equivalent transition for glucose (see above).

The transient response of yeast metabolism to rapid changes in nutrient availability was investigated in several studies. The transient short-term transcriptome and metabolome response of yeast cells to glucose perturbation in continuous cultures was investigated by Kresnowati *et al.*,³ who interpreted the changes at both the transcriptomic and metabolomic levels to reflect two major responses: one involving the transition from fully respiratory to respiro-fermentative metabolism, and the other involving the preparation for an increase in growth rate.³ The transient transcriptional response to switching carbon sources between galactose and glucose was investigated by Ronen and Botstein⁴ and their experimental design proved useful in elucidating the dynamic regulatory networks controlling central carbon metabolism.

In order to investigate nitrogen catabolite repression, ter Schure *et al.*¹⁷ studied the transient response to an ammonium impulse in glutamine-limited yeast cultures. Their study revealed that the ammonium-induced repression did not represent a general stress response but, rather, the relief of ammonium limitation was a specific signal for nitrogen catabolite regulation.

Our previous studies of the transcriptomic responses of yeast cells to the sudden and transient relief of nutrient limitation encompassed both glucose and ammonium responses.⁸ When a glucose impulse was applied to a glucose-limited chemostat culture, we found significant changes in the levels of transcripts related to translation; glucose transport; oxidation/reduction; nucleobase, nucleoside and nucleotide metabolic processes; cell death; aerobic respiration; ion transport; sulphur assimilation; glycolysis; carboxylic acid metabolism; and oxidative phosphorylation. The transcriptomic response of ammonium-limited yeast cells to an ammonium impulse indicated significant changes in the expression of genes involved in translation and its regulation; ribosome biogenesis; non-coding RNA metabolism and processing (including rRNA biosynthesis and maturation); as well as transition metal ion transport. Thus, for both nutrient impulses, there was a response that could be attributed to the increase in growth rate,¹⁸ and another that was specific to the nutrient whose limitation was relieved.¹⁹

In the present study, we have used an integrative approach to map long-term dynamic transcriptome and metabolome data onto metabolic pathways and used such maps to reveal the important molecular events that occur in particular pathways at distinct temporal phases following the transient relief of nutrient limitation. We believe this to be the first study to encompass both the transcriptomic and metabolomic responses of yeast from an initial nutrient-limited steady state, through the period of nutrient excess engendered by a glucose or ammonium impulse, to the re-establishment of

the nutrient-limited steady state. Thus we have followed the complete cycle of famine, feast, and famine to which yeast is thought to be frequently exposed in nature.^{20,21}

Results and discussion

In order to understand the dynamic re-organization of cellular metabolism in response to the sudden and transient relaxation of glucose or ammonium limitation, a systems-based integrative approach, which maps both transcriptome and metabolome data onto metabolic pathways, was used to reveal the key molecular events that occur in specific pathways in distinct time periods following the perturbation. Re-organization of the pathways associated with the central carbon metabolism and energy homeostasis in yeast were given particular attention in this investigation.

Analysis of the time-course data revealed that the transcriptomic response following nutritional perturbations was organized into distinct periods or phases.⁸ The dynamic transcriptional and metabolic responses were clustered into five distinct hierarchical phases in the case of the glucose impulse. These phases, which were formed by the clusters into which the responses fell, reflected the temporal organisation of the total response: the steady-state phase (CP1), the seconds phase (CP2), the minutes phase (CP3), the early-hours response (the first three hours) (CP4) and the late-hours response (the rest of the sampling period) (CP5). On the other hand, a delayed response to the perturbation of the ammonium level was observed rather than the immediate response found for the glucose perturbation. Instead, the phases developed such that the first sample collected (the 20th second sample) was clustered together with the steady states (NP1), the remaining two samples collected in the first minute (40th and 60th seconds) were clustered together with the first two samples collected within the first hour (8th and 16th minutes) (NP2), the remaining two samples collected in the first hour (24th and 32nd minutes) were clustered together with the response obtained in the early hours (the first three hours) (NP3). The rest of the sampling period was clustered together separately from the other phases (NP4) (Fig. 1, ESI 1).

The investigation of the endometabolomic response to the relaxation from carbon-limiting conditions did not display any time dependent organization. Previous findings also revealed that glucose availability played an important role in the arrangement of the endometabolome for different growth rates and glucose-sufficient and -deficient cases could not be clearly separated by means of principal components analysis,¹⁸ implying that yeast is adept at regulating its metabolic flux in response to the external concentration of glucose. During the response to the glucose impulse, the intracellular concentrations of TCA cycle intermediates, sugar derivatives, and amino acids were highest in the later hours following the injection of glucose. At least a 10-fold increase was observed in the concentration of the TCA cycle intermediates, a 3-fold increase in alcoholic derivatives and a 2-fold increase in amino acid concentrations. An accumulation of intracellular amino acid derivatives within the cell was observed as the additional glucose introduced into the medium was depleted and the cells adjusted their metabolism to accommodate the return to a slower growth rate.

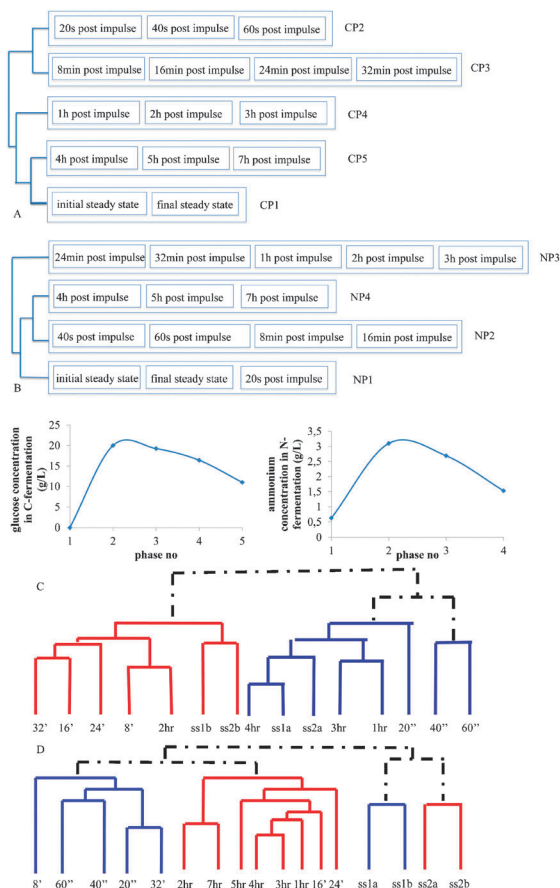


Fig. 1 Hierarchical organization of the transcriptomic response to the impulse like addition of glucose (A) or ammonium (B), the dynamic change in the concentration of the catabolite in its respective culture and the hierarchical clustering of the endometabolome in response to an impulse-like addition of glucose (C) and ammonium (D) into an ammonium-limited culture. The phases corresponding to each cluster are shown as P1, P2, P3, P4 and P5 in (A) and as P1, P2, P3 and P4 in (B).

In response to the impulse-like addition of ammonium, the endometabolome profiles of cells from the nitrogen-limited steady states were clustered together and the samples taken on an hourly basis could be separated in a cluster distinct from that of the samples taken within the first minute. On the other hand, the samples taken within the first hour following the ammonium impulse were distributed between these two clusters (Fig. 1). The dynamic profiles of the intermediary products related to lipid and sphingolipid metabolism, and the phosphatidylinositol signalling pathway displayed a decrease in concentration until NP3, and then recovered as the second steady state was approached. The intracellular concentrations of amino acids and their precursors decreased sharply following the ammonium impulse and recovered gradually as the extracellular ammonium supply gradually became limiting again. The drop in the amino acid concentration in response to ammonium impulse varied between 2-10 fold.

The difference in log. mean values between each response period and the steady-state period (corresponding to fold changes in the transcript and metabolite levels) were calculated for the phases CP2-CP5 in the case of the glucose impulse

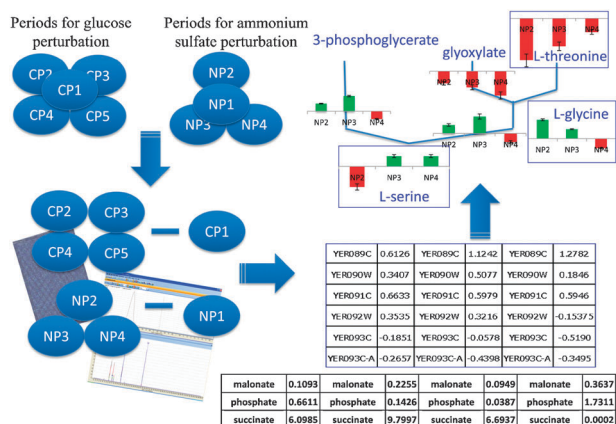


Fig. 2 A schematic overview of the data-overlapping process. The geometric average of log₂ expression values and the arithmetic average of metabolite levels were determined for each phase. The expression values and metabolite concentrations under nutrient limitation were subtracted from the average expression values and the corresponding metabolite concentrations at each phase to determine the net change. The differences in response to the perturbations were determined and mapped on the metabolic pathways.

experiment and for NP2-NP4 in the case of ammonium impulse experiment. These differences were mapped onto the selected metabolic pathways (see Fig. 2 for a summary of the procedure). Consideration of each phase separately enabled a dynamic overview of the cellular decision-making processes involved in pathway selection (Fig. 3).

Changes in the central carbon metabolism

a. Response to the glucose impulse. Introduction of glucose into a carbon-limited steady-state culture evoked changes in the levels of both transcripts and metabolites involved in the TCA cycle, glycolysis, gluconeogenesis, and glycine fermentation pathways. A down-regulation of the genes in the TCA cycle and an up-regulation of the glycolytic genes was observed and the transcriptional re-arrangement of the organism was directed towards ethanol productions. Several other studies have also described a switch towards a respiro-fermentative metabolism within 5 min upon addition of glucose into a continuous culture.^{3,14} A strong and immediate down-regulation of the expression of the glucose utilizing genes; *HXX1*, *HXX2* and *GLK1* was observed upon addition of glucose. This immediate response remains unchanged for nearly an hour post-impulse, although these genes are up-regulated in the later phases of the experiment. Most of the genes that encode enzymes in the lower part of the glycolytic pathway were up-regulated during all phases compared to their expression levels at limiting glucose conditions. Walther *et al.*¹⁴ also reported an increase in the phosphorylated sugars of the glycolytic pathway following the release from glucose limitation, which was congruent with the present findings. From pyruvate, a critical cross-roads metabolite from which the flux may be directed towards either the TCA cycle or the fermentation pathway through the enzymes encoded by *PDC1*, *PDC5* and *PDC6*, the energy metabolism was observed to shift towards fermentation in response to glucose perturbation. The up-regulation in the expression levels of *PDC5* was

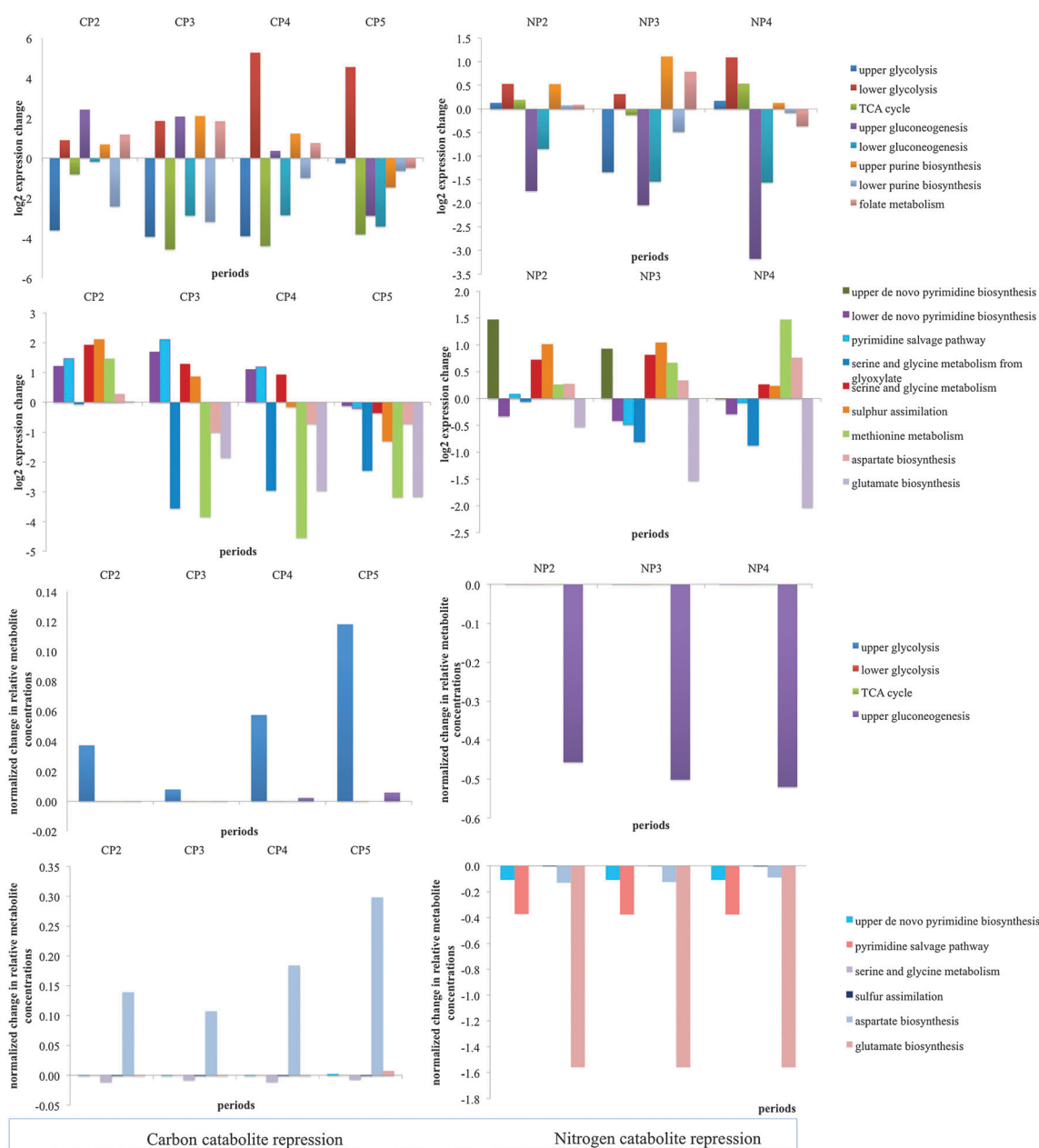


Fig. 3 General trends displaying the changes in the \log_2 expression values of the genes in energy metabolism. The maximum changes in expression levels of the genes in each of the investigated pathways are mapped for each period of either carbon catabolite repression or nitrogen catabolite repression.

strikingly high enabling this shift. Kresnowati M. T. A. P. *et al.*³ also reported an up-regulation of *PDC1* and *PDC6* within 5 min of the addition of glucose into the medium of a carbon-limited culture growing on glucose. The pathway leading to ethanol production was prioritised through the up-regulation of *ADH4* transcription, whereas the expression levels of the other alcohol dehydrogenases; *ADH2*, *ADH3* and *ADH5* remained low throughout the effect of the pulse. A similar down-regulation in *ADH5* expression was previously reported.³ The *ALD* family of genes, involved in directing the relay of transcriptional information from the branch point indicated by acetaldehyde production along the transcriptional relay of information towards the production of

acetic acid, were down-regulated mainly in CP3 and CP4 (Fig. 4, ESI 2).

Most of the genes encoding the enzymes of the TCA cycle were down-regulated throughout the effect of the pulse with the exceptions of the pyruvate carboxylase; *PYC2*, ligases of succinyl Co-A; *LSC1* and *LSC2*, the aconitase; *ACO2*, the malate dehydrogenase; *MDH1* and the isocitrate dehydrogenase; *IDH2*, which were slightly up-regulated in specific phases. *DAL7* of the glyoxylate shunt was strongly up-regulated until CP5. *DAL7* was reported to be involved in allantoin degradation in purine catabolic processes.²² The induction of this gene might have allowed the redirection of flux towards purine catabolism (Fig. 4).

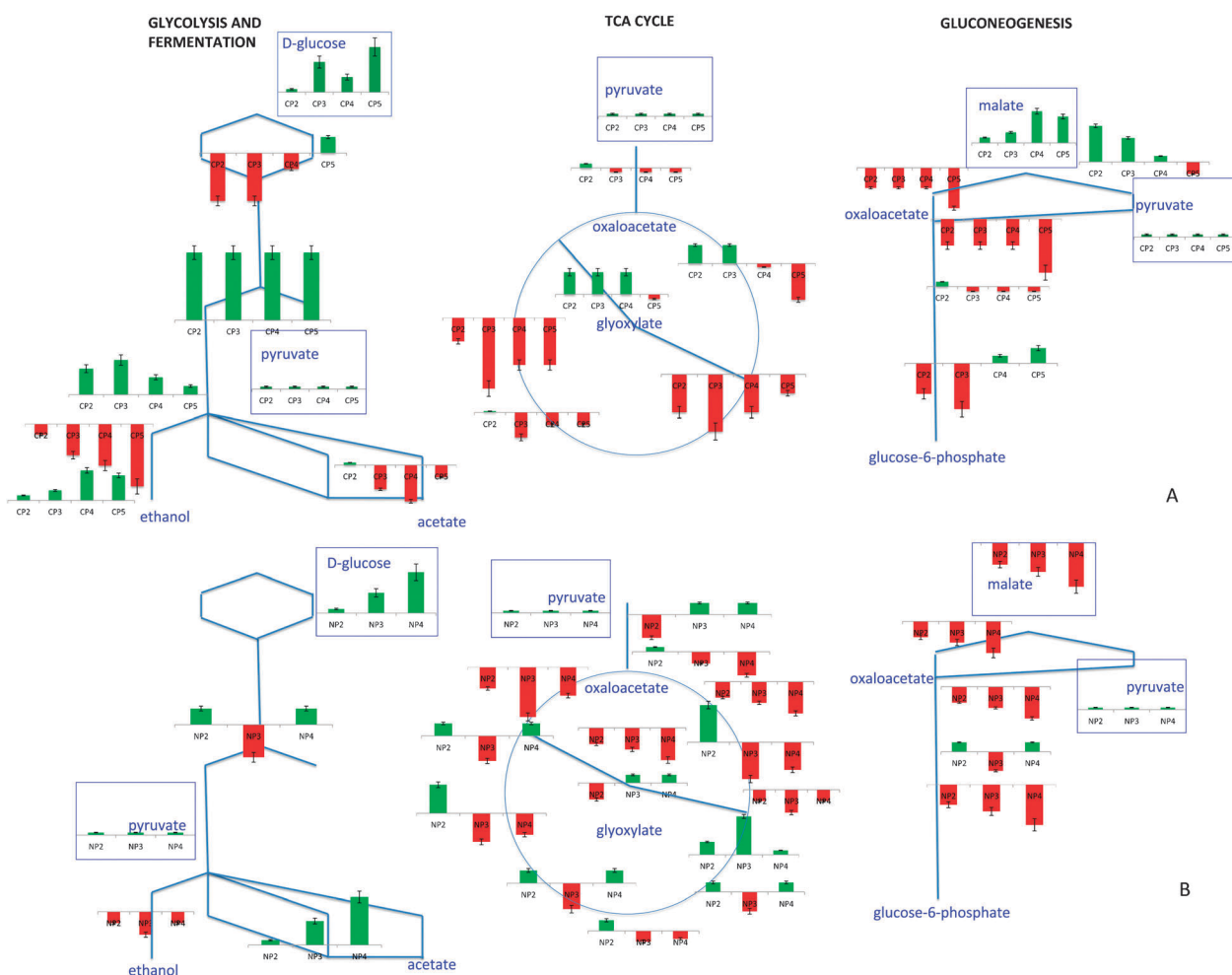


Fig. 4 Dynamic responses in glycolysis, fermentation, the TCA cycle and gluconeogenesis to carbon (A) and nitrogen (B) catabolite repression on representative backbone pathway diagrams. The relative changes in gene expression and metabolite levels with respect to time are denoted in green for up-regulation and red for down-regulation. The expression trend for all the genes in a portion of the pathway is lumped and the average values were taken into consideration. Metabolite names are provided only if that metabolite is an initial or a final product of the pathway or if it is located at a branching point along the pathway. The bars correspond to average values for gene expression and relative metabolite concentration, which are normalized across phases and across two different experimental conditions. Error bars were included to represent the biological variation at each phase. Metabolite plots are enclosed in blue rectangles. The threshold for the significance of the changes in gene expression was selected as $p = 0.01$.

The most pronounced down-regulation of the TCA cycle genes was observed during CP3. The expression levels of genes encoding subunits of the succinate dehydrogenase complex (*SDH1*, *SDH2*, *SDH3* and *SDH4*) were all down-regulated throughout the effective period of the pulse. *SDH1* and *SDH3* were previously reported to be down-regulated during carbon catabolite repression.³ All of the identified and the measured metabolites, namely pyruvate, 2-oxoglutarate, succinate, fumarate and malate displayed slight accumulation in the cells in all periods except for the steady states. This might be the result of the down-regulation of genes that specify enzymes, which use these metabolites as intracellular intermediates (Fig. 4, ESI 3).

MAE1, catalyzing the production of pyruvate from malate, was up-regulated until CP5. The product of the reaction catalyzed by this enzyme, pyruvate, is also a precursor for the synthesis of several amino acids including leucine, isoleucine, valine and alanine in addition to being a key intermediate in

sugar metabolism.²³ Since *PYC1*, whose enzyme product plays a role in the conversion of pyruvate to oxaloacetate, and the malate dehydrogenase *MDH2* were down-regulated throughout the effect of the impulse like addition of glucose and *PYC2* was down-regulated within minutes upon addition of glucose, it could be deduced that pyruvate was used as in the amino-acid production pathways upon relief from the glucose limitation as well as in ethanol production. The down-regulation of malate dehydrogenase (encoded by *MDH2*) and fructose 1,6-bisphosphatase (*FBP1*) upon addition of glucose following a long period of glucose limitation was in accordance with previous findings suggesting the degradation of the enzymes encoded by these genes by a vacuolar pathway²⁴ (Fig. 4, ESI 4).

b. Response to the ammonium impulse. The impulse-like addition of ammonium to a steady-state nitrogen-limited culture also provoked changes in central carbon metabolism (Fig. 4B).

Genes involved in glycolysis were slightly up-regulated in NP2 and NP4 whereas they were down-regulated in NP3. Consequently, the relay of transcriptional information was conveyed towards both ethanol and acetate in NP2 and NP4 following the pyruvate branch point. On the other hand, in NP3, similar to the observations for carbon catabolite repression, a strong down-regulation of the upper glycolytic genes; *HXK1*, *HXK2* and *GLK1* was observed as well as those of the aldehyde dehydrogenases; *ALD4* and *ALD6*, thus limiting the direction of the flow of transcriptional message towards acetate production. Genes encoding the enzymes in the ethanol production pathway were slightly up-regulated in response to the addition of ammonium - except for *ADH2*, which was down-regulated throughout the period in which the impulse is effective (Fig. 4, ESI 2).

The expression levels of the TCA cycle genes were not constitutively up- or down-regulated in response to an ammonium impulse but they rather displayed phase-dependent expression upon relaxation of ammonium limitation. The pyruvate carboxylase; *PYCI* was down-regulated upon the addition of ammonium with the effect on expression increasing in time. On the other hand, *PYC2*, its paralog, was down-regulated immediately at NP2 and was up-regulated in NP3, settling to its steady-state expression level in NP4. One of the genes for citrate synthesis; the dual citrate/methyl-citrate synthase *CIT3* and both malate dehydrogenase genes; *MDH1* and *MDH2* were down-regulated throughout the experiment; whereas the other citrate synthase genes *CIT1* and *CIT2* were only down-regulated in NP3 and NP4, taking more time for their expression levels to decrease. Previous studies indicated a dramatic accumulation of acetate in the absence of *CIT3* through the propionate metabolism in addition to glutamate and alanine. However, it was also reported that this metabolism was affected by *CIT3* only in the absence of glucose or glycerol as the carbon source.²⁵ The presence of glucose as the carbon source in the present study might have prevented an accompanying accumulation of acetate, glutamate or alanine together with the down-regulation of *CIT3*. A gene encoding a putative mitochondrial aconitase, *ACO2*, was slightly up-regulated and that for isocitrate lyase, *ICL1*, was down-regulated throughout the effect of the pulse. On the other hand, *ACO1*, the cytosolic counterpart of *ACO2*, was only up-regulated in NP2 with its expression decreasing in NP3 and NP4 (Fig. 4).

MLS1, enabling the glyoxylate shunt, was down-regulated throughout the effect of the impulse. *MLS1* expression was previously reported as being repressed by glucose.²⁶ During the ammonium perturbation, the constant supply of sufficient glucose, which was probably perceived by the cell as being in excess, would explain the repression of *MLS1*. The malate synthase, *DAL7* was only down-regulated in NP2 and was then up-regulated in NP3 and NP4. It has been reported previously that *DAL7* was repressed under standard growth conditions.²⁷ The introduction of ammonium might have created a temporary situation in which the environment was relieved from all stresses that were created by the limitation of ammonium as well as being supplemented with a sufficient (Or, perhaps, excessive) amount of glucose causing the down-regulation of the expression of that gene in NP2. Ammonium was used up during the course of the fermentation due to

the transiently increased growth rate and the loss by dilution that is intrinsic to continuous culture. Thus the medium gradually shifted back towards the limitation of the nitrogen source. In contrast to the observed during carbon catabolite repression, the intracellular malate concentration was lower following the impulse than it was during limitation during nitrogen catabolite repression. This might be due to the low flux from fumarate and glyoxylate as a result of the down-regulation of *MLS1* and *DAL7* in NP2, *MLS1* and *FUM1* in NP3, and *MLS1* in NP4. This might indicate that *MLS1* may be one of the most important factors determining malate accumulation (Fig. 4, ESI 3).

The expression of the gluconeogenic gene *PCK1*, whose protein product catalyses the conversion of oxaloacetate into phosphoenolpyruvate, decreased upon the addition of ammonium and this down-regulation was stronger in later period in the response to the addition of ammonium. The accumulation of oxaloacetate was prevented by directing the fluxes towards citrate production as an immediate response and the expression levels of the genes encoding the enzymes catalysing this reaction, the citrate synthases; *CIT1* and *CIT2* increased. In NP3 and NP4, however, oxaloacetate accumulation would only be prevented through the activation of the aspartate biosynthetic pathway and the up-regulation of *AAT1* supports this contention. Interestingly, a similar response to the relief from glucose limitation was observed for the malate dehydrogenase *MDH2* and the fructose 1,6 bis-phosphatase *FBP1*. This might indicate that the cells perceived nutrient limitation followed by its abundance through the same mechanisms regardless of the identity of the nutrient; be it glucose or ammonium and this phenomenon requires further investigation (Fig. 4, ESI 4).

Re-organization of the nucleotide pools in response to catabolite repression

The apparent reduction in the concentration of adenine nucleotides associated with the energy homeostasis, which followed the relaxation from nitrogen-limiting conditions in yeast, presents an important problem for our understanding of the mechanisms governing the respiro-fermentative transition. Kresnowati M. T. A. P. *et al.*³ reported that the immediate decrease in adenine nucleotide (AXP) pools following the relief from glucose limitation was not accompanied by changes in the pools for any of the other three nucleotides (NXPs), but rather by the up-regulation of purine biosynthesis, together with C1 and sulphur metabolism. In response to a glucose pulse, the set of genes with a significant change in their expression levels was previously reported to be involved in purine metabolism and the methionine family amino-acid metabolic processes. In our own experiments, clusters of genes that were significantly up-regulated in response to a glucose impulse were found to be enriched with sulphur assimilation process gene ontology terms.⁸ Transient accumulation of the purine salvage pathway intermediates; IMP and inosine were also reported to account for the pronounced drop in the AXP pool by Walther *et al.*¹⁴ in a series of shake-flask cultivations using trehalose to mimic the growth of yeast on glucose-limited medium. The latter investigators suggested that the interconversion

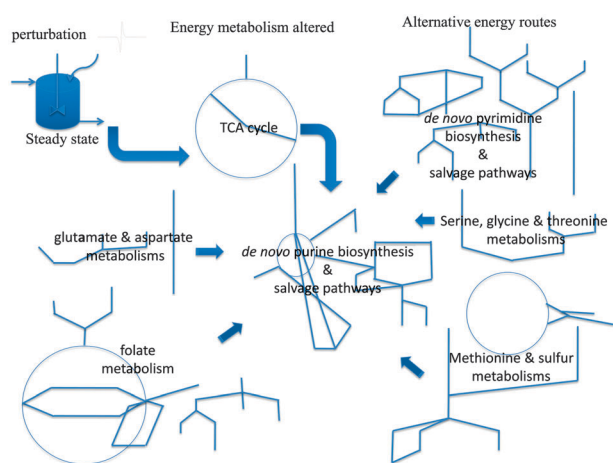


Fig. 5 Re-arrangement of metabolism upon an impulse-like nutritional perturbation. The Figure represents a schematic overview of the response of the energy metabolism to an impulse-like perturbation created by the addition of either glucose or ammonium into their respective limited cultures. The yeast cells found alternative metabolic routes for providing energy precursors through the *de novo* and salvage pathways for purines and pyrimidines. The folate, sulphur amino acid, serine, glycine, aspartate and glutamate metabolisms, which donate C and N atoms for the purine ring, were also affected by this perturbation.

of adenine nucleotides and inosine facilitates the rapid and energy-efficient adaptation of the size of the AXP pool to changing environmental conversions. The accumulation and the recycling of inosine could be considered as a response to energy homeostatic perturbations under fermentative conditions. AXP concentrations were reported to recover quickly to about 80% of their initial levels within 5–10 min, whereas the GXP nucleotide concentration was reported to reach a new steady state that was significantly higher than that prior to the addition of glucose.¹⁴

Consistent with these studies, we also observed significant changes in the expression levels of the genes involved in glycolysis, oxidative phosphorylation, translation, and aspartate family amino-acid metabolic process as a response to the relaxation from both carbon and ammonium limitation.⁸ In the present study, in order to shed light on the mechanisms that counter balance the reduction in AXP pools upon perturbation of energy homeostasis through a pulse injection of a major nutrient, the transcriptomic and the metabolomic data were mapped onto the metabolic pathways that were implicated to be involved in these processes in previous studies (Fig. 5).

Changes in the purine and pyrimidine biosynthetic pathways and their salvage pathways

a. Response to the glucose impulse. Since the tricarboxylic acid cycle becomes inactivated upon addition of glucose, the cells require the activation of alternate routes to satisfy their requirements for the purine nucleotides, ATP and GTP, to sustain the energy metabolism. The initial steps of the *de novo* synthesis of purine nucleotides were immediately activated as soon as glucose was introduced. The immediate up-regulation of the upper purine biosynthetic pathway upon glucose addition may be responsible for the accumulation of IMP,

which was observed by Walther *et al.*¹⁴ This up-regulation was most pronounced during CP3. The observation of the up-regulation in *ADE12*, *ADE13* and *AMD1* during CP2-CP4 indicated that the cyclic conversion of IMP to adenylosuccinate and AMP was possible. On the other hand, the up-regulation of *SAH1*, whose product catalyzes the release of adenine during methyl transfer from S-adenosyl-L-methionine to S-adenosyl-L-homocysteine, and the up-regulation of *ADO1*, which encodes the enzyme that converts adenosine to AMP, may provide an alternative route for the production of AMP. However, the production of ADP from AMP was compromised by the down-regulation of *ADK1* and *ADK2* in CP2. The UMP kinase encoded by *URA6*, up-regulated in this perturbation throughout CP2-CP4, has been reported to compensate for the lack of function in *ADK1*.²⁸ This might have been used as an alternative route for ADP production. *ADK1* and *ADK2* were observed to become progressively up-regulated through CP3-CP5 enabling ADP synthesis from AMP. The accumulated IMP appeared to be converted first to XMP and finally to GMP, based on the transcriptional profiles of the enzymes encoded by the up-regulated *IMD3-IMD4* and *GUA1*, respectively. GMP can then be converted to GDP by the product of *GUK1*, which was observed to be up-regulated at all non-steady state phases of the experiment (Fig. 6).

On the other hand, *YNK1*, encoding the nucleoside diphosphate kinase, catalysing the phosphorylation of ADP and GDP to ATP and GTP, respectively, was found to be down-regulated throughout the experiment. These results indicated that there might be some indirect route for the production of ATP and GTP when the tricarboxylic acid cycle becomes less active upon addition of glucose. One possibility might be an equilibrium shift towards ATP production in the presence of abundant AMP and ADP, through *ADO1*, or the up-regulation of the expression of guanylate kinase, *GUK1* may catalyze the reaction between ADP and GDP to produce ATP. The produced GMP could then be recycled back to xanthosine-5-phosphate through *GUA1*, and thento IMP through *IMD3* and *IMD4* (Fig. 7). Conversions between ADP and dADP, as well as between GDP and dGDP were identified to be active through the up-regulation of the transcription of genes *RNR1*, *RNR2*, *RNR3* and *RNR4* (Fig. 6). Additionally, the up-regulation of *APT1*, *APT2* and *AAH1* may also account for the conversion of AMP to IMP, then *via* adenylosuccinate to adenine and then hypoxanthine. *PNP1*, which specifies purine nucleoside phosphorylase, was also found to be up-regulated. This enzyme catalyzes the reversible reactions between inosine and hypoxanthine as well as between adenine and adenosine. Therefore the accumulation of inosine within 5 min following glucose addition and a delayed accumulation of hypoxanthine within 10 min observed by Walther *et al.*¹⁴ can be explained in the light of these observations (Fig. 6).

Since *HPT1*, encoding an enzyme that catalyses the conversion of hypoxanthine to IMP, was down-regulated at all non-steady state phases of the experiment, there are two possible ways to relieve the accumulation of hypoxanthine. Both of them require the conversion of hypoxanthine to xanthine as the first step and the latter's conversion to uric acid. Although such an enzyme was identified in other fungi, including *Aspergillusniger* and *Yarrowia lipolytica*, the presence of a

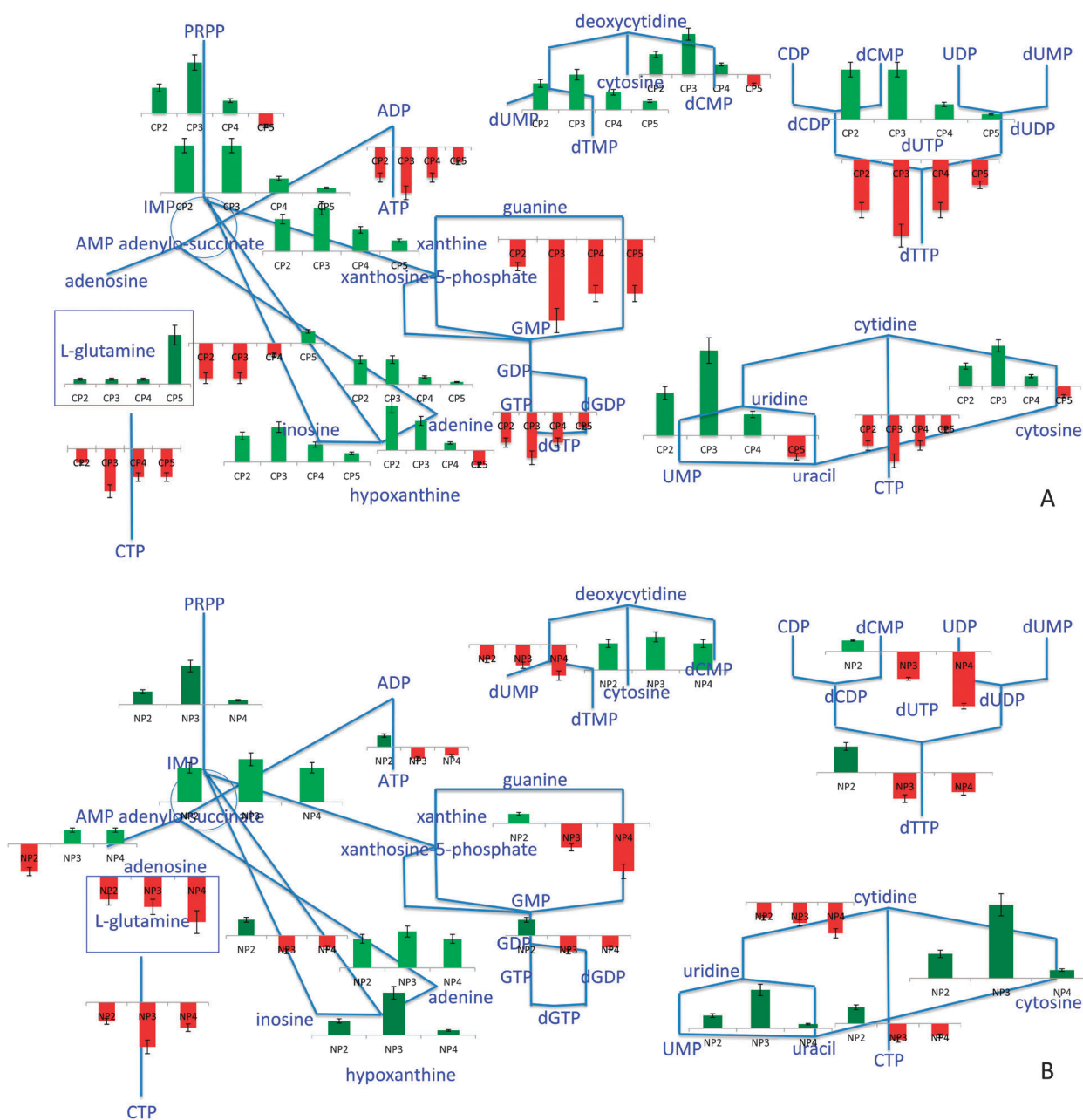


Fig. 6 Dynamic responses in the *de novo* and salvage pathways of purines and pyrimidines to carbon (A) and nitrogen (B) catabolite repression on representative backbone pathway diagrams. See the legend to Fig. 4 for a further explanation of the representation.

similar enzyme could not be demonstrated in *S. cerevisiae*. A BLAST search of the *S. cerevisiae* genome²⁹ using the amino-acid sequences of An03g01530, An04g05440 and 1.17.1.4 enzymes did not indicate the presence of any similar sequences in *S. cerevisiae*. However, it should be noted that the reactions of the purine salvage pathway in yeast have not been completely identified.³⁰ Walther *et al.*,¹⁴ for instance, included a similar potentially relevant reaction in the purine salvage pathway in *S. cerevisiae* based on the experiments that they have carried out using several *psp* mutants. Since the conversion of xanthine to XMP was not possible due to the down-regulation of *XPT1*, fluxes should be oriented from xanthine towards 5-ureido-4-imidazole carboxylate and later to glycine to be used in the superpathway to serine, threonine and glycine.

However, the detailed mechanisms and the enzymes catalyzing these reactions are, as yet, unknown. Another alternative route utilizing xanthine and hypoxanthine is purine catabolism, enabling the degradation of the purine compounds into uric acid, allantoin, urea and (later) into ammonium through the utilization of the gene products of *DAL1*, *DAL2*, *DAL3* together with *DUR1*, 2.³¹ *DAL1* and *DUR1*, 2 were up-regulated at all non-steady state phases of the experiment. *DAL2*, on the other hand, was down-regulated at all non-steady state phases of the experiment and *DAL3* was up-regulated in CP2, CP4 and CP5, but was down-regulated in CP3. The reaction through Dal3p caused the accumulation of glyoxylate during the production of ammonium. As previously stated, a member of the glyoxylate shunt, Dal7p, may also take role in purine

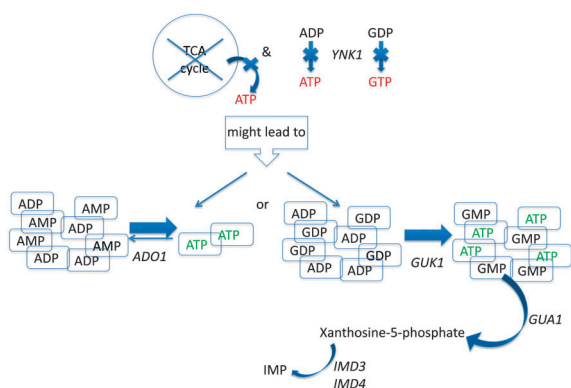


Fig. 7 Schematic overview of alternative routes for ATP production during inactivation of the TCA cycle and the down-regulation of *YNK1*. Alternative routes that could be used to generate ATP in response to the impulse-like addition of glucose into the fermentation medium, inactivating the TCA cycle as well as causing the down-regulation of *YNK1*.

catabolic processes^{22,32} and *DAL7* was observed to be up-regulated during carbon catabolite repression (Fig. 6, ESI 5).

In CP5, almost all of the purine biosynthetic pathway components were down-regulated and, since the TCA cycle became active again, the ATP production necessary for respiration and maintenance would be supplied through that channel (Fig. 6, ESI 5).

The *de novo* biosynthesis of pyrimidine ribonucleotides UTP and CTP from L-glutamine was reduced, due to the observed down-regulation of *URA3* upon introduction of glucose into the steady-state glucose-limited culture. This effect, which was observed from the transcriptomic data, was persistent throughout the effective duration of the impulse. It was previously reported that the UXP and CXP profiles displayed a similar decrease in concentration to those observed for AXP and GXP pools upon the addition of glucose into its respective limited culture.³ Although the genes encoding the enzymes involved in the conversion of L-glutamine into orotidine-5'-phosphate and the gene expression the minor orotate phosphoribosyltransferase isozyme, *URA5*, were all up-regulated, the *de novo* biosynthetic pathway of pyrimidines appeared to be blocked by the down-regulation of *URA3* throughout the phases during which the effect of the impulse-like addition of glucose persisted. This result may indicate that the *de novo* synthesis of UMP was reduced under these conditions. The up-regulation of *URA6*, mediating the conversion of UMP to UDP, also the up-regulation of *FUR1*, mediating the conversion of uracil to UMP may suggest the activation of the salvage pathway of pyrimidine nucleotides for the utilization of uracil, which was provided in the fermentation medium. *FUR4*, encoding uracil permease that mediates the uptake of uracil, was observed to be up-regulated in CP2 and CP3 and became down-regulated in CP4 and CP5. The presence of uracil was reported to result in the activation of uracil phosphoribosyltransferase (UPRTase) encoded by *FUR1* and the repression of genes involved in the pyrimidine biosynthesis.³³ The genes, which are associated with the pyrimidine salvage pathway, were found to be up-regulated through CP2-CP4, with expression peaking in CP3. The conversion of UDP and

CDP to UTP and CTP was also compromised by the down-regulation of *YNK1* in CP2-CP4. However, *URA7* and *URA8*, whose gene products catalyze the conversion of UTP to CTP, were activated during CP2-CP5. Additionally, *DUT1*, encoding the enzyme which catalyzes the conversion of dUTP to dUMP, was up-regulated (ESI 6, ESI 7).

Alternative routes for the production of UTP and CTP are therefore required. One of two possibilities to overcome this obstacle would be the presence of as yet undefined gene products compensating for the role of *YNK1*. The other alternative may be an equilibrium shift among XDPs and XTPs to favour XTP generation in times of cellular need. The flux from UDP might be split, with some being used for the generation of ATP that, in turn, could be used for the conversion of UDP to UTP and further to CTP. It is interesting to note that although uracil was provided in the medium to ensure that it was always present in excess to compensate for the auxotrophy of the strain, the salvage pathways of pyrimidine biosynthesis was still responsive to the impulse-like addition of glucose to the fermentation medium, and hence to increased growth rates. Previous studies reported increased transcription of genes from the pyrimidine pathway with increased growth rate¹⁸ and the findings of the present study accord with this (Fig. 6).

b. Response to the ammonium impulse. In response to the introduction of ammonium into a nitrogen-limited culture, the genes taking role in the *de novo* synthesis of purine nucleotides, as well as the salvage pathways for purines and their nucleosides, were up-regulated immediately in NP2 except for *ADE16*, *XPT1* and *RNR3*. The upper purine biosynthetic pathway remained up-regulated through periods NP2-NP4, similar to what has been observed during carbon catabolite repression. This is most pronounced in NP3, which is later than in glucose repression. The genes that were required for the synthesis of ADP during NP2-NP4 were also up-regulated. The observation of up-regulation of *IMD4*, *GUA1* and *GUK1* indicated that GDP may also be synthesized during NP2-NP4. One of the most pronounced changes in NP3 was observed in the down-regulation of *YNK1* taking a role in the production of XTPs from XDPs and dXDPs in a similar, but delayed, response to that of carbon catabolite repression of metabolism. As the effect of the impulse of ammonium began to be lost in NP4, the up-regulation of the genes in upper purine biosynthetic pathway became less pronounced (Fig. 6, ESI 5).

The effect of the addition of ammonium into a nitrogen-limited culture was observed to cause similar but less pronounced changes in the *de novo* synthesis of pyrimidine ribonucleotides pathway than the response to the addition of glucose to a C-limited culture. The most-pronounced down regulation in the *de novo* synthesis of pyrimidine ribonucleotides pathway was observed in the expression level of *URA3* and, similar to the observation for the response to glucose impulse, the step catalysed by Ura3p may be a bottleneck, limiting the production of UMP, the precursor for the production of UTP and CTP. *URA7* and *URA8*, whose products catalyze the conversion between UTP and CTP were both up-regulated in NP2 and NP4 whereas only *URA8* was down-regulated in NP3. The salvage pathway of pyrimidine deoxyribonucleotides was

also not as strongly affected in response to the ammonium perturbation as it was following the introduction of glucose (Fig. 6, ESI 6, ESI 7).

Changes in the folate metabolism

a. Response to the glucose impulse. The role of folates in metabolism is to donate 1C units to various biosynthetic pathways through the production of tetrahydrofolate (THF), which is an active form of folic acid.³⁴ Carbons C2 and C8 of purine rings are obtained from the metabolism of folate that takes place in the mitochondria.³⁵ *FOL1* and *FOL2*, whose products take part in the upper folate biosynthetic pathway starting from GTP, were up-regulated in CP2-CP4. The formation of 1C units was enabled through the interconversions between THF, 5,10-methylene-THF and 5,10-methenyl-THF. The expression levels of the genes encoding the enzymes facilitating these interconversions were up-regulated in CP2 and CP3 and these paths gradually became inactive through CP4 and CP5. The conversion of glycine and THF into 5,10-methylene-THF, NH_3 and CO_2 was facilitated by the active glycine cleavage complex (Lpd1p, Gcv1p, Gcv2p and Gcv3p). All members except for *LPD1* were observed to be up-regulated in CP2-CP4. *LPD1* was previously reported to be down-regulated in response to catabolite repression and its release from repression requires the activity of the Hap2/3/4/5 complex.³⁶ Additionally, *SHM1* and *SHM2*, which encode enzymes in the superpathway of serine and glycine biosynthesis, facilitated the conversion of serine and THF into glycine and 5,10-methylene-THF.³⁴ Glycine was reported to donate the nitrogen at the N7 position of purine rings and their carbon atoms at the C4 and C5 positions.³⁵ The folate metabolism switched back to the steady-state configuration as the amount of glucose became progressively limited in CP5 (Fig. 8, ESI 8).

b. Response to the ammonium impulse. In response to the addition of ammonium to an N-limited culture, the genes involved in the folate biosynthetic pathways and the folate interconversions were up-regulated in NP2 and NP3. The expression levels of the genes of the pathway were up-regulated except for those of *LPD1*, *ABZ2* and *CDC21*, which were down-regulated. The interconversions among folate products were active throughout NP2-NP3 enabling the generation of 1C species to be utilized in purine biosynthetic processes. More genes were down-regulated in NP4 (Fig. 8, ESI 8).

Changes in the superpathway of serine and glycine biosynthesis, sulphur amino acid metabolic pathways, the aspartate biosynthetic pathway and the superpathway of glutamate biosynthesis

a. Response to the glucose impulse. The genes whose products mediate the interconversion of L-threonine and L-glycine in the superpathway of serine and glycine biosynthesis were up-regulated, as soon as glucose was introduced into the carbon-limited culture. *SHM2* and *SHM1*, which both encode the enzyme that catalyzed the interconversion between L-glycine and L-serine, were found to be up-regulated throughout CP2-CP4, and down-regulated in CP5. A slightly increased accumulation L-serine and L-threonine was also observed through CP3-CP5. One route leading to the synthesis of L-glycine that from glyoxylate, was observed to be rendered congested through the down-regulation of *AGX1* throughout the experiment. This down-regulation was most pronounced in CP3 and CP4 (Fig. 9, ESI 9).

In response to carbon catabolite repression, methionine biosynthesis was up-regulated in CP2 and CP3 *via* the route utilizing sulphate rather than L-aspartate. Genes with a role in the upper biosynthetic pathway were gradually down-regulated

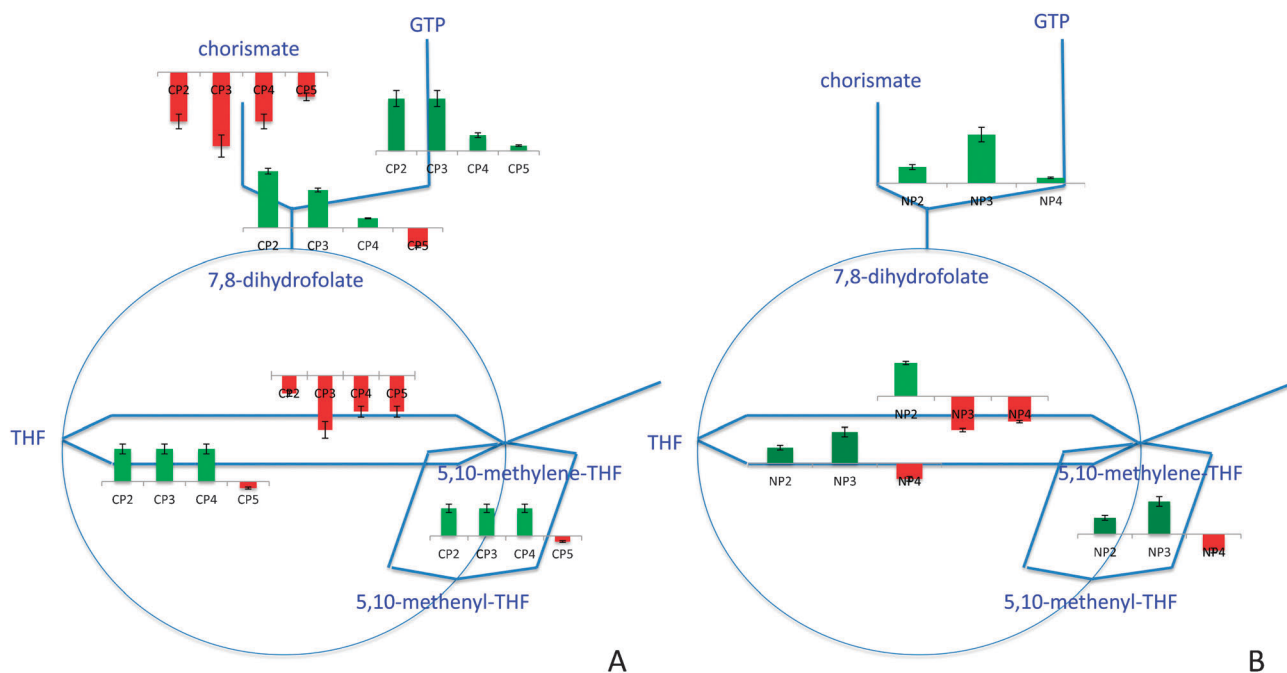


Fig. 8 Dynamic response in folate metabolism to carbon (A) and nitrogen (B) catabolite repression on representative backbone pathway diagrams. See the legend to Fig. 4 for a further explanation of the representation.

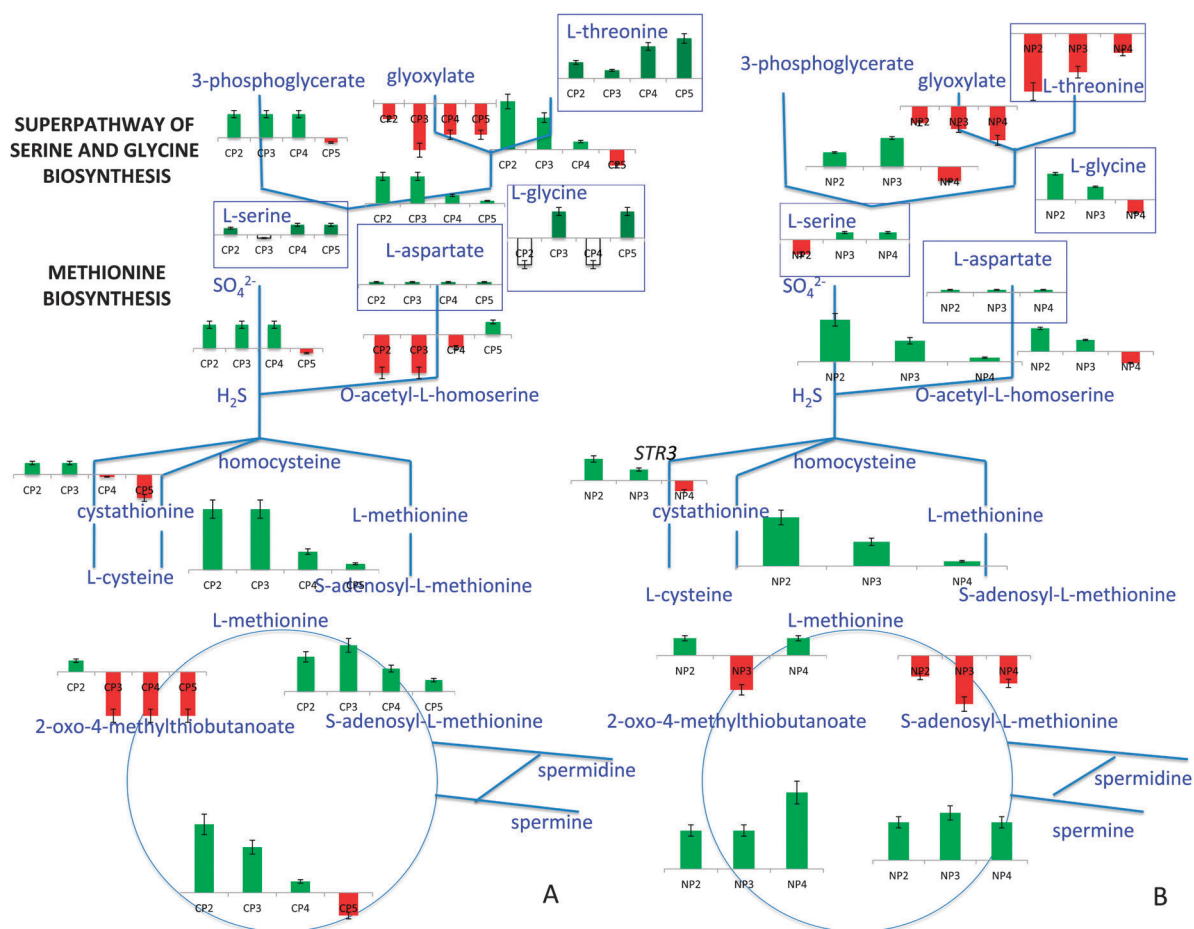


Fig. 9 Dynamic response in the superpathway of serine and glycine and the methionine biosynthetic pathway to carbon (A) and nitrogen (B) catabolite repression on representative backbone pathway diagrams. See the legend to Fig. 4 for a further explanation of the representation.

in CP4 and CP5. The only exception for up-regulation was observed for *MET17*, which was down-regulated at all post-impulse periods, and may create a bottleneck for the formation of L-methionine. A close paralog, *CYS3* (BLASTP e-value: $5.7e-35$), might have replaced its function, allowing continued flux through the pathway. L-cysteine was converted to homocysteine and then to L-methionine through the up-regulation of *CYS3* and *STR3*. *SAM1*, *SAM2* and *MET6* (on the route towards L-methionine and S-adenosyl-L-methionine) were up-regulated once homocysteine was produced. The enzyme product of the up-regulated *MET6*, enabling L-methionine production from L-homocysteine, also facilitated the interconversion between 5-methyl-THF and THF. The direction of fluxes from S-adenosyl-L-homocysteine towards L-homocysteine was facilitated through the up-regulation of *SAH1*, enabling the release of additional adenosine for the production of AMP in purine biosynthesis (Fig. 9, ESI 9).

Genes in the salvage pathway of methionine were up-regulated immediately. Genes of this pathway became progressively down-regulated through CP3 to CP5. The down-regulation in the genes of the salvage pathway was the most pronounced in CP5. Among these genes, the methylthioadenosine phosphorylase, *MEU1* was previously reported to regulate the expression of *ADH2*, for which the strongest down-regulation of expression was also observed in CP5³⁷ (Fig. 9, ESI 9).

Aspartate biosynthesis donates the nitrogen in the N1 position of the purine ring.³⁵ In response to carbon catabolite repression, the expression levels of the genes in the aspartate biosynthetic pathway were not reduced immediately but remained active through CP2, being down-regulated in CP3-CP5. During CP2, although *PYC1* was down-regulated, its paralog *PYC2* was still up-regulated, enabling the formation of oxaloacetate then to be down-regulated throughout CP3-CP5. The down-regulation in the cytosolic aspartate aminotransferase, encoded by *AAT2*, and the up-regulation in the mitochondrial aspartate aminotransferase, specified by *AAT1*, indicated that L-aspartate biosynthesis from oxaloacetate was preferred through the mitochondrial, rather than the cytosolic, route. However, the route for the production of homoserine and L-threonine from aspartate was reduced (as a result of the down-regulation of the pathway genes *HOM2-HOM6* and *THR4*, respectively) throughout the experiment. The accumulated aspartate would be converted to fumarate by the catalytic action of the up-regulated *ADE12* and *ADE13* (through adenylosuccinate), or by the up-regulated *ARG1* and *ARG4* (through L-argininosuccinate). The accumulation of fumarate throughout the effective period of the impulse-like addition of glucose also supported this hypothesis.

Another possibility would be the conversion of L-aspartate to N-carboxyl-L-aspartate through the up-regulated *URA2* to

shift the fluxes towards pyrimidine biosynthetic metabolism. The cyclic interconversion between L-aspartate and L-asparagine was also facilitated through the enzymes of the up-regulated *ASN1* and *ASN2* during CP2-CP5. The gene expression levels of the asparaginases mediating the conversion of L-asparagine to L-aspartate and ammonia (donating a nitrogen atom for the purine ring) were also up-regulated during all post-impulse phases. The intracellular concentrations of L-aspartate, homoserine and L-threonine were all high and the down-regulation of the genes whose enzymes take role in the pathway from L-aspartate and homoserine towards L-threonine production was accompanied by this intracellular accumulation (Fig. 10, ESI 10).

L-glutamine delivers the nitrogen atoms at positions N3 and N9 of the purine ring.³⁵ L-glutamine biosynthesis initiates from a component of the TCA cycle, isocitrate. The conversion of isocitrate into 2-oxoglutarate through the catalysis by the product of *IDP1*, which was selectively up-regulated throughout the period of carbon catabolite repression, allowed further alpha-ketoglutarate to be used in biosynthetic processes.³⁸ 2-oxoglutarate, together with NH₃ would then be converted into L-glutamate through the catalysis of the up-regulated glutamate dehydrogenases, and 2-oxoglutarate would be converted *via* the up-regulated glutamate synthase *GLT1* in CP2.

This process was observed to be down-regulated during CP3-CP5. The utilization of ammonia and its conversion into L-glutamine were diverted through glutamine synthetase (Gln1p) during CP2 and CP3; however, the expression of *GLN1* was reduced during CP4 and CP5. The intracellular concentrations of ammonia, 2-oxoglutarate, L-glutamate and L-glutamine were all high throughout the catabolite repression (Fig. 10, ESI 10).

b. Response to the ammonium impulse. Upon relaxation of ammonium limitation, the expression levels of the genes in the superpathway of serine and glycine biosynthesis were up-regulated in NP2 and NP3 except for the alanine:glyoxylate aminotransferase *AGX1*, which was slightly down-regulated in NP2 and even more so in NP3, reducing the production of L-glycine from glyoxylate. L-serine production from either branch was reduced in NP4 due to the down-regulation of the genes catalysing the enzymes along the pathways (Fig. 9, ESI 9).

Genes encoding enzymes in both upper branches of the methionine biosynthetic pathway, utilizing either sulphate or L-aspartate, were up-regulated in response to an ammonium perturbation. The down-regulation of *MET17* during NP3 would be compensated by *CYS3* as was found

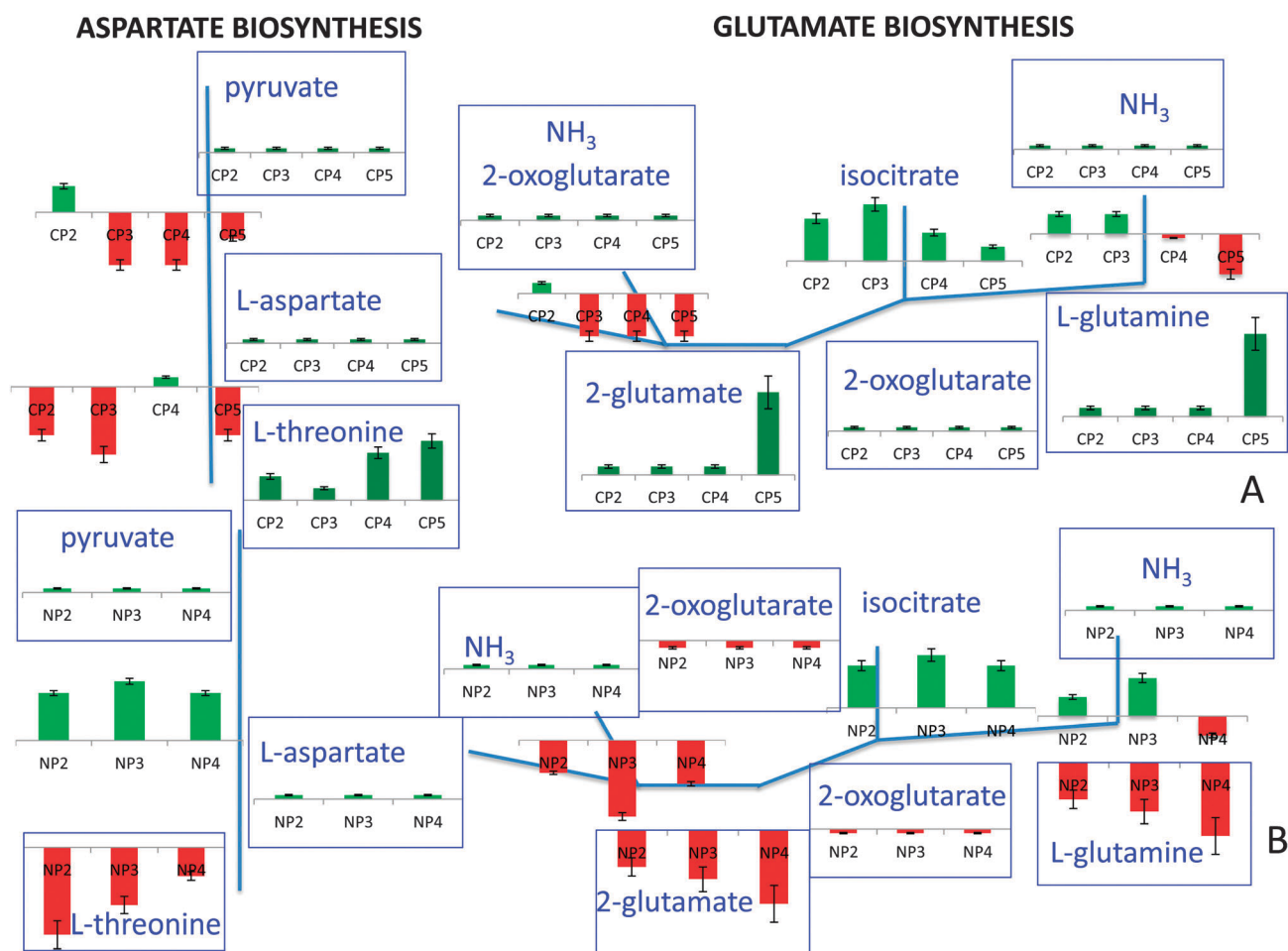


Fig. 10 Dynamic response in aspartate and glutamate biosynthesis to carbon (A) and nitrogen (B) catabolite repression on representative backbone pathway diagrams. See the legend to Fig. 4 for a further explanation of the representation.

for the glucose perturbation. The low expression levels that were observed for *MET2* or *STR3* indicated that the production of L-methionine from L-aspartate or from L-cysteine, respectively, was reduced. The genes in the salvage pathway of methionine were up-regulated throughout nitrogen catabolite repression except for the branched-chain amino acid transferase *BAT2* and the aromatic aminotransferase II, Aro9p, and this pathway remained functional in NP4 just before regaining the steady-state as opposed to the down-regulation of the pathway genes observed towards exiting carbon catabolite repression (Fig. 9, ESI 9).

Nitrogen catabolite repression resulted in an up-regulation of the genes acting in the biosynthesis of L-aspartate from pyruvate; the response increasing gradually from NP2 to NP4. The two genes encoding the isoforms of pyruvate carboxylase (*PYC1* or *PYC2*) were active at all periods, and L-aspartate production was enabled through either the mitochondrial or the cytosolic aspartate aminotransferase during NP2-NP4. In contrast to what was observed during carbon catabolite repression, homoserine and L-threonine production were also up-regulated during NP2-NP4. The intracellular concentrations of L-aspartate and homoserine were high, whereas that of L-threonine was low in accordance with the observation of the up-regulation of the pathway components from L-aspartate and homoserine towards L-threonine (Fig. 10, ESI 10).

The expression levels of the genes involved in the production of L-glutamate were observed to be low during NP2-NP4, which was also observed in the intracellular concentration of the metabolite itself in response to the impulse-like addition of ammonium. Although the NADP-specific isocitrate dehydrogenase *IDPI*, which encodes the enzyme that mediates the conversion of isocitrate to 2-oxoglutarate, was up-regulated, the genes encoding glutamate dehydrogenases (*GDH1*, *GDH2* and *GDH3*) were down-regulated in NP2 and NP3. The direct conversion of 2-oxoglutarate into L-glutamate was reduced by the down-regulation of *GLT1* in NP2 but induced in NP3 and NP4 as a result of the up-regulation in the expression level of the gene. L-glutamine production from L-glutamate was active as a response to nitrogen catabolite repression in NP2-NP3 but not in NP4. The intracellular concentrations of ammonia, 2-oxoglutarate and L-glutamine were all high (Fig. 10, ESI 10).

Materials and methods

Data acquisition

The dynamic transcriptome data were obtained from chemostat experiments in response to a nutritional perturbation⁸ in pre-processed form. cDNA synthesis and double-stranded cDNA retrieval was carried out as described in the Affymetrix GeneChip[®] Expression Analysis Technical Manual, using appropriate kits. Biotin-labelled cRNA was synthesized and was purified using clean up kits. Hybridization and loading onto Affymetrix Yeast2 arrays were carried out as described in the GeneChip[®] Expression Analysis Technical Manual. The chips were then loaded into a fluidics station for washing and staining using Microarray Suite 5 with EukGe W S2v4 programme. Lastly, the chips were loaded onto the Agilent GeneArray scanner 2500 and another quality check was performed using Microarray Suite 5.

In compliance with MIAME guidelines,³⁹ the microarray data from this study has been submitted to ArrayExpress at the European Bioinformatics Institute under accession number E-MTAB-643. Full details of sampling and the transcriptome analysis were reported previously.⁸

Sampling and extraction of the endometabolome, analytical methods for fingerprinting

For metabolic fingerprinting, 5 ml of sample were rapidly quenched in 60% (v/v) methanol buffered with tricine at $-50\text{ }^{\circ}\text{C}$ and the endometabolites were extracted in boiling 75% (v/v) ethanol buffered with tricine at $80\text{ }^{\circ}\text{C}$ as described by Castrillo *et al.*⁴⁰ The vacuum-dried samples were stored at $-80\text{ }^{\circ}\text{C}$ until analysis. For both footprinting and fingerprinting, derivatization and identification of peaks *via* GC-ToF-MS were performed as described by Pope *et al.*⁴¹ A total of 69 metabolites were semi-quantitatively identified in the analysis among the 118 peaks that were detected for the case of the glucose impulse whereas 64 metabolites were identified among the 155 peaks that were detected in response to an impulse like addition of ammonium into its limited culture. The samples for GC-MS analysis were spiked with $100\text{ }\mu\text{l}$ 0.18 mg ml^{-1} succinic d₄ acid as the internal standard and the peak areas were normalized against the standard. The dynamic metabolome data are provided in ESI 11.

Identification of gene expression in co-clustered time spans and mapping of the transcriptome and the metabolome on metabolic pathways

The hierarchical clustering of the transcriptome and the metabolome data was carried out using Hierarchical Clustering Explorer (HCE) 3.0⁴² with the distance measure selected as the Pearson correlation. Average linkage method was used in the construction of the dendrogram. All data was row normalized prior to analysis with mean 0 and standard deviation 1. The periods were identified from the determined clusters. The gene expression levels in each period were statistically confirmed to display insignificant differences within a single period using the Student's t-test with a significance threshold of 0.05. The geometric means of the logarithm-transformed expression levels in each period were then calculated. The differences in logarithmic mean values for the periods following a perturbation and the period consisting of the succeeding or preceding steady-state data (expressed as fold changes either in expression or in the amount of the measured metabolite) were mapped onto the metabolic pathways. Consideration of each period separately enabled the dynamic overview of the decision-making involved in the pathway preferences.

The complementary nature of the transcriptome and the endometabolome data was investigated by mapping expression levels and intracellular metabolite concentrations simultaneously onto metabolic pathways (SGD, <http://pathway.yeastgenome.org:8555/expression.html>). The direction and the reversibility of the reactions were assessed using the KEGG database⁴³ and the Yeast 4.0 model.⁴⁴

Conclusion

The quantification of the dynamic changes in the yeast transcriptome and metabolome in response to an impulse-like perturbation in nutrient availability and the integration of

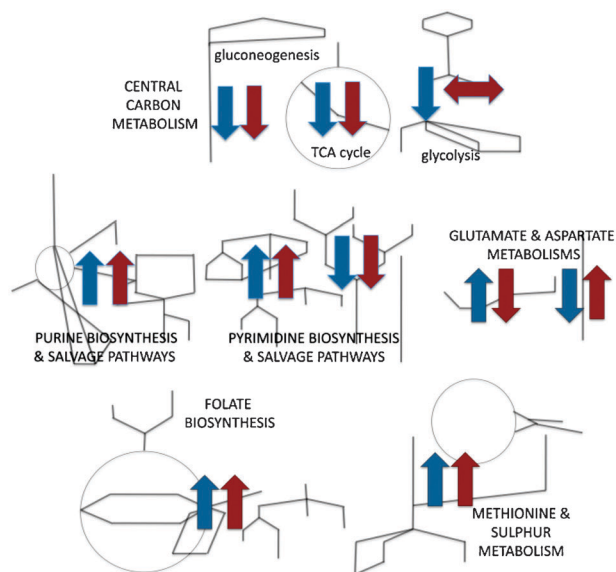


Fig. 11 Schematic summary of the main metabolic changes following glucose and ammonium impulses. The main changes in response to glucose perturbation were displayed in blue and those in response to ammonium perturbation were displayed in burgundy. The up-arrow indicates an overall increase in metabolic activity in a particular pathway and a down-arrow indicates an overall decrease. The left-right arrow indicates that the pathway was mostly unresponsive to the perturbation.

these data with metabolic pathway information revealed the long-term dynamic re-organization of yeast metabolism (Fig. 11).

The glycolytic and gluconeogenic pathways and the TCA cycle were all affected by a glucose impulse injected into a carbon-limited culture, and different members of paralogous pairs of genes encoding isozymes involved in the central energy metabolism were observed to be active at different phases of the response to the perturbation. The transcriptional response of the genes involved in the upper glycolytic pathway was immediate and these genes remained down-regulated for at least three hours, limiting glucose phosphorylation to avoid glucose-accelerated death. The most pronounced down-regulation of the TCA cycle genes was observed within the first hour following the glucose impulse, displaying a rather late response. The impulse-like addition of ammonium into an N-limited culture triggered an even later response than that to the addition of glucose. The response observed in the lower glycolytic pathway was found to be glucose-specific as an equivalent response was not observed during the ammonium perturbation. The fluxes towards the lower gluconeogenic pathway were limited through the down-regulation of the genes encoding specific enzymes in both cases.

The initial steps in the *de novo* synthesis of purine nucleotides were immediately activated as soon as glucose was introduced. Upon depletion of glucose, almost all of the pathway components were down-regulated and, with the activation of the TCA cycle, the necessary energy for survival and maintenance would again be supplied through that channel. The time-dependent changes observed in the purine salvage pathway provided additional evidence about the role and organization of this pathway to control energy homeostasis and

compensate for the sudden drop in the AXP pools. Further insight was provided into the accumulation of inosine, IMP, and hypoxanthine that had been reported in previous studies. The *de novo* biosynthesis of pyrimidine ribonucleotides was also reduced with the introduction of glucose into a C-limited culture. The salvage pathway of pyrimidine nucleotides was activated for the utilization of uracil, which was supplemented in the fermentation medium due to the auxotrophic requirement of the yeast strain under study. The effect of the addition of ammonium to an N-limited culture was observed to cause similar, but less pronounced, changes in both the *de novo* synthesis of pyrimidine ribonucleotides and their salvage pathways to those observed in the response to the addition of glucose under C-limitation.

The folate interconversions donating 1C units in purine metabolism were active during the first hour following the introduction of glucose, being gradually down-regulated until the effect of the impulse ceased to exist. A very similar pattern of regulation to what had been observed for the carbon catabolite repression was encountered in the first three hours following the addition of ammonium. The pathway gradually became inactive as the effect of the impulse began to cease.

In response to carbon catabolite repression, our integrative analysis of the methionine biosynthetic pathways indicated the prominence of sulphur metabolism, rather than that of L-aspartate. The direction of flux was re-arranged such that the release of additional adenosine was facilitated. Genes in the salvage pathway of methionine were also observed to be up-regulated immediately. All of the upper methionine biosynthetic pathway genes were up-regulated in response to an ammonium perturbation. A similar pattern was observed for the genes in the salvage pathway of methionine to that of the biosynthetic pathway, except that this pathway remained functional until the return to the steady state.

In response to carbon catabolite repression, the down-regulation of L-aspartate biosynthetic pathway genes was delayed, being prominent after the first minute. An accumulation of L-aspartate would have been relieved by its conversion to fumarate through various routes. Another possibility would have been its re-direction towards pyrimidine metabolism. In contrast, nitrogen catabolite repression resulted in an increasing up-regulation in the L-aspartate biosynthetic pathway in response to the rapid introduction of ammonium. L-glutamine production was up-regulated throughout the period of carbon catabolite repression, diverting alpha-ketoglutarate to biosynthetic processes, and was down-regulated throughout the period of nitrogen catabolite repression.

This long-term integrative study revealed that, in addition to the dynamic re-organization of the *de novo* biosynthetic pathways, the salvage pathways appeared to be re-organized in a time-dependent manner by catabolite repression in yeast. The transcriptional and metabolic responses observed for nitrogen catabolite repression were not as severe as those for carbon catabolite repression. This may have been due to the fact that uracil, histidine, and leucine were supplemented in the fermentation medium to satisfy the auxotrophic requirements of the strains employed. Selective up- or down regulation of different members of paralogous pairs of genes throughout the response to the relaxation from nutritional

limitation in yeast requires further investigation to assign specific functions to the isozymes encoded by such gene pairs. Although this study provided additional information on inosine accumulation and recycling, it has also indicated the requirement for further studies to shed light on specific phenomena such as the relief of the accumulation of hypoxanthine or the down-regulation of *YNK1*, whose product phosphorylates XDP nucleotides to XTP.

Transcriptome and metabolome data were observed to complement each other, providing useful information whenever they were simultaneously available. Additional metabolite measurements and studies at the proteome and phosphoproteome level, complemented by accurate measurements of mRNA decay, may provide better information to shed light onto the time-dependent re-organization of yeast cells as a dynamic response to a changing nutritional environment and thus provide a quantitative understanding of cell behaviour. Similar integrative systems-level approaches would also provide a solid understanding of metabolic processes that control the respiro-fermentative transition in human cells.

Acknowledgements

The authors greatly acknowledge the financial support for the research from the BBSRC (Grant BB/C505140/1 to SGO), and the travel grants for DD kindly provided by the Research Council of Turkey (TUBITAK) through the BDP programme and the Turkish State Planning Organization DPT09K120520. The research was also financially supported by Bogazici University Research Fund through Project No 631 and TUBITAK through Project No 106M444. Further support came from European Commission through the Coordination Action Project YSBN (Contract No.018942 to both BK and SGO) and UNICELLSYS Collaborative Project (No. 201142 to SGO).

Notes and references

- 1 D. Y. Shin, K. Matsumoto, H. Iida, I. Uno and T. Ishikawa, *Molecular and Cellular Biology*, 1987, **7**(1), 244.
- 2 L. Viladevall, R. Serrano, A. Ruiz, G. Domenech, J. Giraldo, A. Barcelo and J. Arino, *J. Biol. Chem.*, 2004, **279**(42), 43614.
- 3 M. T. A. P. Kresnowati, W. A. van Winden, M. J. H. Almering, A. ten Pierick, C. Ras, T. A. Knijnenburg, P. Daran-Lapujade, J. T. Pronk, J. J. Heijnen and J. M. Daran, *Mol. Syst. Biol.*, 2006, **2**, 49.
- 4 M. Ronen and D. Botstein, *Proc. Natl. Acad. Sci. U. S. A.*, 2006, **103**(2), 389.
- 5 E. Braun and N. Brenner, *Phys. Biol.*, 2004, **1**, 67.
- 6 J. van den Brink, P. Daran-Lapujade, J. T. Pronk and J. H. de Winde, *BMC Genomics*, 2008, **9**, 100.
- 7 A. P. Gasch, P. T. Spellman, C. M. Kao, O. Carmel-Harel, M. B. Eisen, G. Storz, D. Botstein and P. O. Brown, *Molecular Biology of the Cell*, 2000, **11**, 4241.
- 8 D. Dikicioglu, M. E. Karabekmez, B. Rash, P. Pir, B. Kirdar and S. G. Oliver, *BMC Syst. Biol.*, 2011, **5**, 148.
- 9 H. C. Causton, B. Ren, S. S. Koh, C. T. Harbison, E. Kanin, E. G. Jennings, T. I. Lee, H. L. True, E. S. Lander and R. A. Young, *Molecular Biology of the Cell*, 2001, **12**, 323.
- 10 H. Moriya and M. Johnston, *Proc. Natl. Acad. Sci. U. S. A.*, 2004, **101**(6), 1572.
- 11 M. C. M. Meijer, J. Boonstra, A. J. Verkleij and C. T. Verrips, *J. Biol. Chem.*, 1998, **273**(37), 24102.
- 12 J. M. Gancedo, *Microbiology and Molecular Biology Reviews*, 1998, **62**(2), 334.
- 13 S. Zaman, S. I. Lippman, L. Schneper, N. Slonim and J. R. Broach, *Molecular Systems Biology*, 2009, **5**, 245.
- 14 T. Walther, M. Novo, K. Rössger, F. Létisse, M. O. Loret, J. C. Portais and J. M. François, *Mol. Syst. Biol.*, 2010, **6**, 344.
- 15 B. Magasnik, *Eukaryotic Cell*, 2003, **2**(5), 827.
- 16 B. Magasnik and C. A. Keiser, *Gene*, 2002, **290**, 1.
- 17 E. G. ter Schure, H. H. W. Silje, E. E. Vermeulen, J. W. Kalthorn, A. J. Verkleij, J. Boonstra and C. T. Verrips, *Microbiology*, 1998, **144**, 1451.
- 18 J. I. Castrillo, L. A. Zeef, D. C. Hoyle, N. Zhang, A. Hayes, D. J. C. Gardner, M. J. Cornell, J. Petty, L. Hakes, L. Wardleworth, B. Rhash, M. Brown, W. B. Dunn, D. Broadhurst, K. O'Donoghue, S. S. Hester, T. P. J. Dunkley, S. R. Hart, N. Swainston, P. Li, S. J. Gaskell, N. W. Paton, K. S. Lilley, D. B. Kell and S. G. Oliver, *J. Biol.*, 2007, **6**, 4.
- 19 A. Gutteridge, P. Pir, J. I. Castrillo, P. D. Charles, K. S. Lilley and S. G. Oliver, *BMC Biol.*, **8**, 68.
- 20 C. Zeyl, *FEMS Microbiol. Lett.*, 2004, **233**, 187.
- 21 M. P. Zustiak, J. K. Pollack, M. R. Marten and M. J. Betenbaugh, *Curr. Opin. Biotechnol.*, 2008, **19**, 518.
- 22 S. H. Yoo, F. S. Genbauffe and T. G. Cooper, *Molecular and Cellular Biology*, 1985, **5**(9), 2279.
- 23 E. Boles, P. de Jong-Gubbels and J. T. Pronk, *Journal of Bacteriology*, 1998, **180**(11), 2875.
- 24 G. C. Hung, C. R. Brown, A. B. Wolfe, J. Liu and H.-L. Chiang, *J. Biol. Chem.*, 2004, **279**(47), 49138.
- 25 E. B. Graybill, M. F. Rouhier, C. E. Kirby and J. W. Hawes, *Arch. Biochem. Biophys.*, 2007, **465**, 26.
- 26 M. A. van den Berg, P. de Jong-Gubbels and H. yde Steensma, *Yeast*, 1998, **14**, 1089.
- 27 M. Kunze, I. Pracharoenwattana, S. M. Smith and A. Hartig, *Biochim. Biophys. Acta, Mol. Cell Res.*, 2006, **1763**, 1441.
- 28 R. Schrickler, V. Magdolen, A. Kaniak, K. Wolf and W. Bandlow, *Gene*, 1992, **122**-1, 111.
- 29 A. Goffeau, B. G. Barrell, H. Bussey, R. W. Davis, B. Dujon, H. Feldmann, F. Galibert, J. D. Hoheisel, C. Jacq, M. Johnston, E. J. Louis, H. W. Mewes, Y. Murakami, P. Philippsen, H. Tettelin and S. G. Oliver, *Science*, 1996, **274**(546), 563.
- 30 M. Kaneisha, M. Araki, S. Goto, M. Hattori, M. Hirakawa, M. Itoh, T. Katayama, S. Kawashima, S. Okuda, T. Tokimatsu and Y. Yamanishi, *Nucleic Acids Res.*, 2008, **36**, D480.
- 31 R. Fluri and J. R. Kinghorn, *Curr. Genet.*, 1985, **9**, 573.
- 32 E. Fernandez, M. Fernandez and R. Rodicio, *FEBS Lett.*, 1993, **320**(3), 271.
- 33 J. E. Kurtz, F. Exinger, P. Erbs and R. Jund, *Curr. Genet.*, 2002, **41**, 132.
- 34 K. E. Christensen and R. E. MacKenzie, *BioEssays*, 2006, **28**, 595.
- 35 D. H. Griffin, in *Fungal Physiology*, Wiley, 2nd edn, 1996.
- 36 S. B. Bowman, Z. Zaman, L. P. Collinson, A. J. Brown and I. W. Dawes, *Molecular and General Genetics*, 1992, **231**(2), 293.
- 37 A. L. Subhi, P. Diegelman, C. W. Porter, B. Tang, Z. J. Lu, G. D. Markham and W. D. Kruger, *J. Biol. Chem.*, 2003, **278**(50), 49868.
- 38 R. J. Haselbeck and L. McAlister-Henn, *The Journal of Biological Chemistry*, 1993, **268**(16), 12116.
- 39 A. Brazma, P. Hingamp, J. Quackenbush, G. Sherlock, P. Spellman, C. Stoeckert, J. Aach, W. Ansorge, C. A. Ball, H. C. Causton, T. Gaasterland, P. Glenisson, F. P. C. Holstege, I. F. Kim, V. Markowitz, J. C. Matese, H. Parkinson, A. Robinson, U. Sarkans, S. Schulze-Kremer, J. Stewart, R. Taylor, J. Vilo and M. Vingron, *Nat. Genet.*, 2001, **29**, 365-371.
- 40 J. I. Castrillo, A. Hayes, S. Mohammed, S. J. Gaskell and S. G. Oliver, *Phytochemistry*, 2003, **62**, 929.
- 41 G. A. Pope, D. A. MacKenzie, M. Defemez, M. A. M. M. Aroso, L. J. Fuller, F. A. Mellon, W. B. Dunn, M. Brown, R. Goodacre, D. B. Kell, M. E. Marvin, E. J. Louis and I. N. Roberts, *Yeast*, 2007, **24**, 667.
- 42 J. Seo, M. Bakay, Y. W. Chen, S. Hilmer, B. Shneiderman and E. P. Hoffman, *Bioinformatics*, 2004, **20**, 2534.
- 43 M. Kanehisa and S. Goto, *Nucleic Acids Res.*, 2000, **28**(1), 27.
- 44 P. D. Dobson, K. Smallbone, D. Jameson, E. Simeonidis, K. Lanthaler, P. Pir, C. Lu, N. Swainston, W. B. Dunn, P. Fisher, D. Hull, M. Brown, O. Oshota, N. J. Stanford, D. B. Kell, S. G. Oliver, R. D. Stevens and P. Mendes, *BMC Syst. Biol.*, 2010, **4**, 145.